

AN ANALYTICAL MODEL OF LONG-WAVELENGTH AVALANCHE PHOTODIODE (APD) BASED ON $\text{InAs}_{1-x}\text{Sb}_x$ FOR FREE SPACE OPTICAL COMMUNICATION APPLICATIONS

P. K. Maurya¹, P. Chakrabarti²

¹National Technical Research Organisation, Government of India, Block-III,
Old JNU Campus, New Delhi, (India)

²Department of Electronics Engineering, Indian Institute of Technology,
Banaras Hindu University, Varanasi, (India)

ABSTRACT

In the present paper, a generic numerical model of a long-wavelength avalanche photodiode (APD) based on narrow bandgap semiconductor InAsSb on InAs substrate is reported. This model has been applied for theoretical characterization of a proposed $N^+ \text{InAs/P-InAsSb}$ avalanche photodiode structure for possible application in 2-5 μm wavelength region. The parameters such as gain, excess noise factor and their trade-off with variation of doping concentration and bias voltage have been estimated for the APD taking into account history-dependent theory of avalanche multiplication process. The long-wavelength avalanche photodiode is expected to find application in free space optical communication system and optical gas sensor.

Keywords: *Avalanche Photodiode (APD), Excess Noise Factor, Free Space Optical Communication (FSO), Multiplication Gain.*

I. INTRODUCTION

Free space optical communication (FSO) represents one of the most promising approaches for addressing the emerging broadband access market. In the recent years, free space optical communication has drawn considerable interest in commercial and military applications due to high available bandwidths, portability and high security of systems. The other advantages of free space optical communication over optical fiber communication include quick link set up, rapid deployment time, license- and tariff-free bandwidth allocation, low power consumption etc. FSO system can offer up to 100 Gb/s data rates between two points [1]. These systems are also compatible to a wide range of other communication system and are sufficiently flexible so as to be easily implemented using a variety of different architectures. Several researchers have already established that infrared region is best suited for free space optical communication [2]-[6]. InAsSb based long-wavelength infrared (LWIR) photodetectors operating in the 2-5 μm spectral range find application in free space optical communication. In free space optical communication system, photodetector is the key component in the receiver unit. Successful implementation of free space optical communication receiver at these wavelengths requires development of suitable photodetectors operating at these wavelengths. Long-wavelength infrared semiconductor photodetectors also find a variety of non-telecommunication applications. As the long-

wavelength region contains the fundamental fingerprint absorption bands of a pollutant and toxic gases, the LWIR photodetectors are very attractive use in optical gas sensors [7]-[10]. The gas sensing instrumentation can be greatly simplified by making use of multiplication photodetector such as an avalanche photodiode (APD). The dominating mid-infrared photodetector materials include IV-VI and II-VI alloys such as PbSe, HgCdTe and III-V alloys such as InAs, InSb and their related ternary and quaternary alloys. Because of some inherent difficulties with IV-VI and II-VI materials, the ternary III-V alloy InAsSb eventually emerged as potentially the most promising material for application in mid-infrared region. The energy bandgap of $\text{InAs}_{1-x}\text{Sb}_x$ vary with composition from 0.4 eV (77 K) to 0.1 eV (300 K) making it attractive for use in the 3-5 μm and 8-13 μm spectral range, respectively. The advantage of InAsSb over the other material include higher electron and hole mobilities, high-quality and low cost substrate. The performance of such devices is strongly influenced by several factors which are special to narrow band gap semiconductors. The operation of such devices is highly restricted by the requirement of low temperature operation.

Among various photodetectors, an APD offers a very high sensitivity because of its internal gain mechanism, but at the same time it has more noise compared with its non-multiplying counterpart because of the randomness in the avalanche multiplication process which is responsible for the gain of APD. Before history-dependent theory was proposed, it was assumed that ionization coefficient of electrons and holes are functions only of the local value of the electric field [11], [12] which is a poor approximation for photodiodes that have very short multiplying regions. As pointed out by Okuto and Crowell [13]-[15] and others, a carrier starting with near zero energy, relative to band edge, will have an almost zero chance of having an ionization collision until it has gained sufficient energy from the electric field to attain the necessary energy to permit impact ionization. The local-field model works well at low electric fields at which mean free path between ionizing collisions is long compared with the dead length [17]. However, at high electric fields at which the reciprocal of the ionization coefficient is comparable to or even less than the dead length, a theory that assumes all holes or all electrons have the same probability of ionization, irrespective of where they were created, can lead to considerable error [16]. In this paper we have applied history-dependent ionization model for charactering a long-wavelength APD theoretically.

II. THEORETICAL MODEL

The structure under consideration is $\text{N}^+ - \text{InAs} / \text{P} - \text{InAsSb}$ heterojunction APD as shown in Fig.1(a). The energy band diagram of the structure is shown in Fig.1 (b).

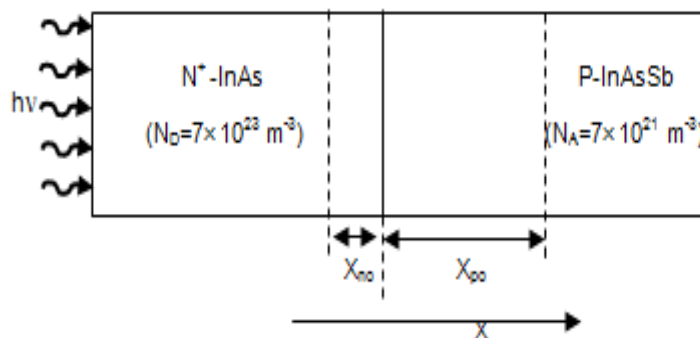


Fig.1 (A): Schematic Diagram of the Avalanche Photodetector Structure

The InAsSb layer is intended to be used as the light absorption region. The proposed APD structure under consideration is supposed to be grown on In As substrate. The N⁺-P junction is used to create a narrow multiplying region. The photogenerated carriers in the narrow bandgap InAsSb material undergo avalanche multiplication before being collected at the output terminals. The theoretical characterization of the detector has been carried out in respect of multiplication gain (M) and excess noise factor F(M) of the APD at 77K using the history-dependent theory of impact ionization.

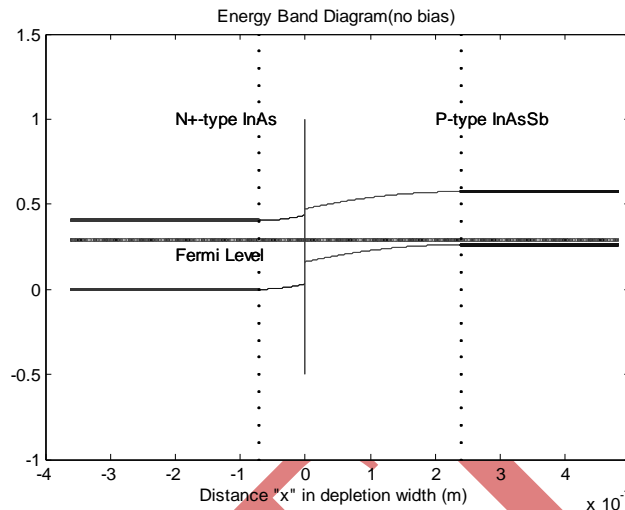


Fig.1(b): Energy band diagram

2.1 Local Field Theory: The equation governing the electron and hole current distributions at any point x in the avalanche multiplication region can be written as

$$\frac{di_p(x)}{dx} = -\frac{di_n}{dx} = \alpha(x)i_n(x) + \beta(x)i_p(x) + g_0(x) \quad (1)$$

where $g_0(x)$ is the sum of the thermal and optical current generation rate, α and β are electron and hole ionization coefficients, respectively, which are functions of electric field at the point x . For steady state these equations are easily solved to find the multiplication gain at any point x as [11]

$$M(x) = \frac{\exp\left[-\int_0^{x_0} (\alpha - \beta) dx\right]}{1 - \int_0^W \alpha \exp\left[-\int_0^x (\alpha - \beta) dx\right] dx} \quad (2)$$

If the only carriers injected into depletion layer are holes then the excess noise factor for holes is given by [10]

$$F_P = M_P \left[1 + \left(\frac{1-k}{k} \right) \left(\frac{M_P - 1}{M_P} \right)^2 \right] \quad (3)$$

and for electrons

$$F_n = M_n \left[1 - (1-k) \left(\frac{M_n - 1}{M_n} \right)^2 \right] \quad (4)$$

if the only injected carriers are electrons. where $k = \beta/\alpha$ is constant, α and β are the ionization coefficients of electrons and holes, respectively and M_n and M_p are the electron and hole multiplication factors respectively.

2.2 Gain Theory of History-Dependent Ionization Coefficient: In the case of history dependent ionization coefficient, the position dependent gain can be obtained by considering an electron-hole pair generated at x' and calculating the ensemble average of the total number of resulting electrons and holes generated in a single event involving a primary electron or hole. An electron which encounters an ionizing collision at x creates two cold electrons and a cold hole which create further carriers. A hole also undergoes multiplication in a similar manner. The multiplication gain at position x' due to impact ionization considering the contributions of both electrons and holes can be obtained as [17]

$$M(x') = \frac{N_e(x') + N_h(x')}{2} \quad (5)$$

where $N_e(x')$ and $N_h(x')$ are respectively the average number of carriers in the two chains generated by the initial electron and hole injected at x' separately given by [14]

$$N_e(x') = P_{se}(x'|0) + \int_0^{x'} N_e(x'|x) \cdot p_e(x'|x) dx \quad (6a)$$

$$N_h(x') = P_{sh}(x'|w) + \int_{x'}^w N_h(x'|x) \cdot p_h(x'|x) dx \quad (6b)$$

Where

$$N_e(x'|x) = \langle n_e(x'|x) \rangle = 2N_e(x) + N_h(x) \quad (7a)$$

and

$$N_h(x'|x) = \langle n_h(x'|x) \rangle = 2N_h(x) + N_e(x) \quad (7b)$$

Here $n_e(x'|x)$ and $n_h(x'|x)$ are the total numbers of electrons and holes generated in a single trial initiated by a primarily electrons and holes respectively; $P_{se}(x'|0)$ and $P_{sh}(x'|w)$ are the survival rates of electrons and holes having carrying carrier ionization probability densities of $p_e(x'|x)$ and $p_h(x'|x)$ respectively, which are given by

$$p_e(x'|x) = \alpha(x'|x)P_{se}(x'|x) \quad (8a)$$

$$p_h(x'|x) = \beta(x'|x)P_{sh}(x'|x) \quad (8b)$$

The excess noise factor can be expressed as [17]

$$F(x') = \frac{\left\langle \left(\frac{N_e(x') + N_h(x')}{2} \right)^2 \right\rangle}{M^2(x')} \quad (9)$$

2.3 Numerical Technique: In this computation it has been assumed that the ionization coefficient of an electron or a hole not only depends on the local electric field but also on the location of the point x' where it is created and the field profile at all points between x' and x . The computation starts with estimation of the local electric field $E(x)$. The local electric field value is subsequently used to determine the effective electric field $E_{eff,e}(x'|x)$ and $E_{eff,h}(x'|x)$ between x and x' by considering the history dependent factor by using following equations.

$$E_{eff,e}(x'|x) = E \times \operatorname{erf}\left(\frac{(x' - x)}{\lambda_e}\right) \quad (10a)$$

$$E_{eff,h}(x'|x) = E \times \operatorname{erf}\left(\frac{(x - x')}{\lambda_h}\right) \quad (10b)$$

$$\lambda_e(E) = \frac{l_e}{\operatorname{erf}^{-1}\left(\frac{b_e}{b_e + E \log(2)}\right)} \quad (11a)$$

$$\lambda_h(E) = \frac{l_h}{\operatorname{erf}^{-1}\left(\frac{b_h}{b_h + E \log(2)}\right)} \quad (11b)$$

where l_e and l_h are the dead lengths of electron and holes respectively and E is the value of local electric field.

Using these values of the effective electric field the history dependent ionization coefficients $\alpha(x'|x)$ and $\beta(x'|x)$ in the multiplication region; the ionization probabilities $p_e(x'|x)$ and $p_h(x'|x)$ are computed assuming the survival probabilities $p_{se}(x'|x)$ and $p_{sh}(x'|x)$ of the electrons and holes are equal to one.

These values are used for computation of $N_e(x')$ and $N_h(x')$ by iteration technique subjected to boundary conditions

$$N_e(0) = 0 \text{ and } N_h(0) = 1$$

In order to have the desired accuracy the conservative convergence criterion (relative error $< 10^{-4}$) was used. The multiplication gain and excess noise factors were computed numerically using equations (5) and (9) respectively.

III. RESULT AND DISCUSSION

The numerical calculations have been performed on an N^+ -InAs/P-InAs_{1-x}Sb_x operated in mid infrared region operated at 77K. The incident photons with energy lower than bandgap of InAs cross the N^+ region with negligible absorption and get absorbed mostly in the narrow bandgap InAs_{0.88}Sb_{0.12} region creating electron-hole pairs. The following forms of the local field-dependent ionization coefficients were used in numerical computation [14].

$$\alpha(E) = A_n \exp\left(-\frac{B_n}{|E|}\right) \quad (12)$$

$$\beta(E) = A_p \exp\left(-\frac{B_p}{|E|}\right) \quad (13)$$

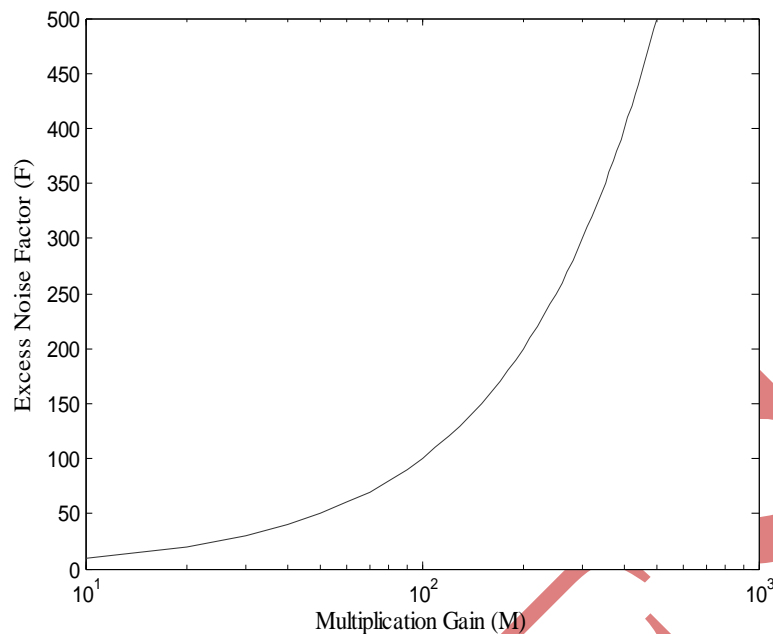


Fig.2- Variation of Effective Electric Field within Depletion Region

Fig. 2 shows the variation of effective electric field with distance x in the depletion region. The maximum value of electric field is attained at the junction (at $x=0$). It decreases non-linearly as we move either side of the junction. The maximum value of electric field is 3.5×10^6 V/m at $x=0$ which is attained at reverse bias voltage 9 V. The dependence of total multiplication gain where an electron hole pair is generated or injected in the depletion region at different reverse voltage is shown in Fig.3. It is seen that the multiplication gain of the APD remains low up to a reverse voltage very close to breakdown and increases very fast at breakdown. The low multiplication gain up to 80-90% of the breakdown voltage is accounted for the low tunneling current at heterointerface. The multiplication gain of the APD is estimated to be 398 at $x=1.5 \times 10^{-8}$ m which is attained at reverse bias voltage 9.2V. It is also seen that for a constant multiplication gain when reverse breakdown voltage increase, distance in multiplication region decreases accordingly.

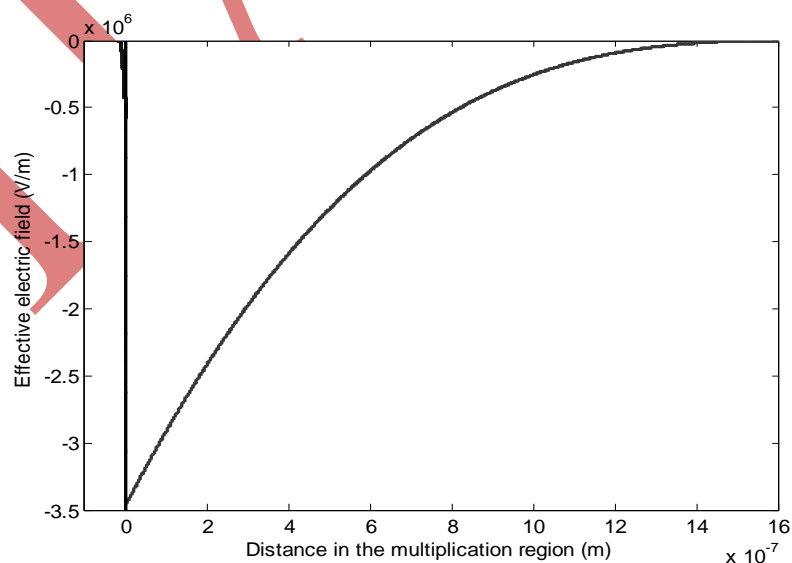


Fig. 3: Net Multiplication Gain within the Avalanche Multiplication Layer Thickness with Varying Doping Concentration

Table 1: Various Parameters Used In Computation

Parameters	Values
T	77 K
X	0.12
N_A	$5.0 \times 10^{24} \text{ m}^{-3}$
N_D	$5.0 \times 10^{22} \text{ m}^{-3}$
$\chi_p(\text{InAs})$	4.9 eV [15]
$\chi_n(\text{InAs}_{1-x}\text{Sb}_x)$	$(4.9-0.31x) \text{ eV}$ [15]
$E_g(\text{InAs})$	0.354 eV
$E_g(\text{InAs}_{1-x}\text{Sb}_x)$	$0.411 - \frac{3.4 \times 10^{-4} T^2}{T+210} - 0.876x + 0.7x^2 - 3.4 \times 10^{-4} x(1-x)T \text{ eV}$ [18]
$m_p(\text{InAs})$	$0.41 m_0$ [18]
$m_n(\text{InAs}_{1-x}\text{Sb}_x)$	$(0.023-0.039x+0.03x^2) m_0$ [18]
$\epsilon_p(\text{InAs})$	$15.15 \epsilon_0$ [18]
$\epsilon_n(\text{InAs}_{1-x}\text{Sb}_x)$	$(15.15+1.65x) \epsilon_0$ [18]
A_n	$0.7 \times 10^8 (\text{m}^{-1})$
A_p	$6.0 \times 10^7 (\text{m}^{-1})$
B_n	$1.5 \times 10^8 (\text{Vm}^{-1})$
B_p	$1.75 \times 10^7 (\text{Vm}^{-1})$

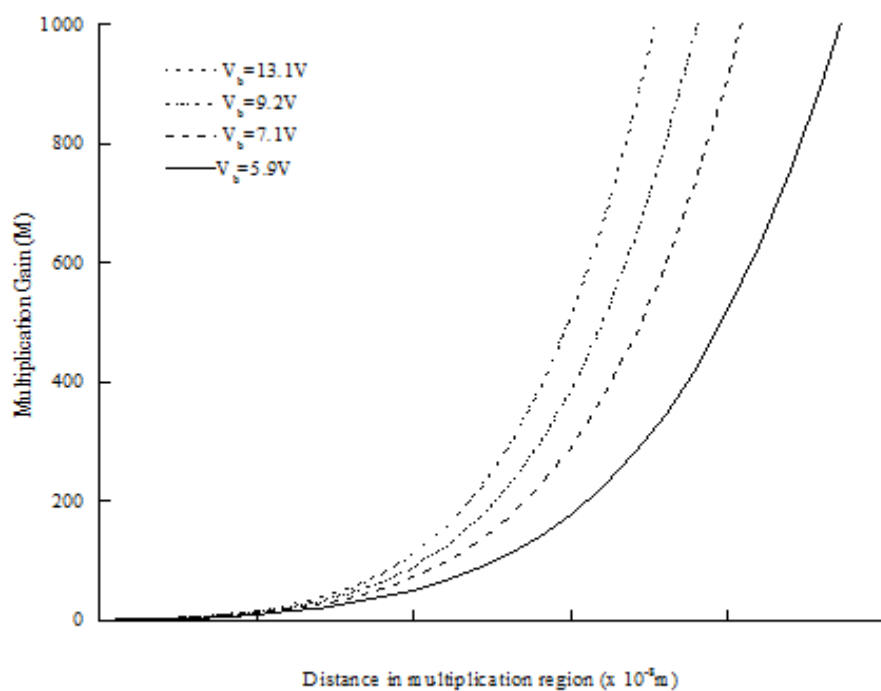


Fig. 4: Excess Noise Factor with Electron Multiplication Gain with Varying Doping Concentration Using Local Field Theory

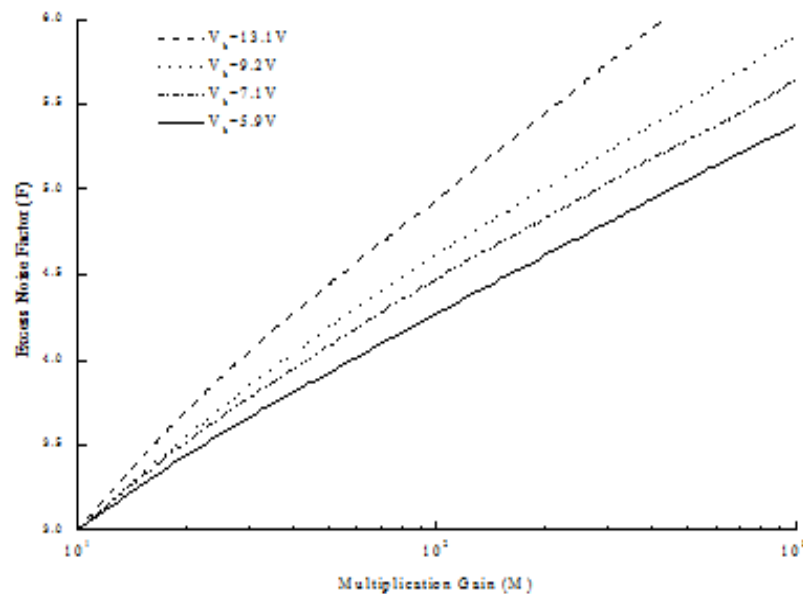


Fig.5: Excess-Noise Factor with Multiplication Gain with Varying Doping Concentration Using History-Dependent Theory

Fig. 4 shows the variation of excess noise factor with electron multiplication gain. It is seen that the excess noise factor increases sharply with electron multiplication gain. The actual multiplication gain depends on effective ionization coefficient of a carrier which in turn not only depends upon the electric field $E(x)$, but also on location of the point at which the carrier was created on the field profile between x (point of creation) and x' (point of successful ionization). The excess noise factor calculated from the expression (9) and (10) is plotted in Fig.5 for various electron multiplication gains at different reverse voltage. In this figure, it can be seen that excess-noise factor increases with electron multiplication gain. The excess noise factor of the APD is 98 when multiplication gain and reverse voltage are 100 and 9.2V respectively. The figure depicts that for a constant multiplication gain, excess noise factor increase with increase in reverse voltage.

IV. CONCLUSION

Free space optical communication is the up-to-date technology for security and high available bandwidth of systems. A long-wavelength APD has been simulated to determine the electrical and optical characteristic of the device. The simulation is based on gain theory of history dependent ionization coefficient. The device can be operated at a suitable breakdown voltage to provide a high multiplication gain. The proposed device is expected to find application in free space optical communication systems.

REFERENCES

- [1] Andrew Hood, Allan Evans and Manijeh Razegh, "Type-II Superlattices and Quantum Cascade Lasers for MWIR and LWIR Free-Space Communications", *Proc. of SPIE*, 6900, pp. 690005(1-9), 2009.
- [2] H. Manor and S. Arnon, "Performance of an optical wireless communication system as a function of wavelength", *Appl. Opt.*, vol. 42, pp. 4285–4294, 2003.

- [3] N.S. Kopeika, J. Bordogna, "Background noise in optical communication systems", *Proc. IEEE*, vol. 58, pp. 1571–1577, 1970.
- [4] H. Henniger and O. Wilfert, "An Introduction to free-space optical communication", *Radioengineering*, Vol. 19, No. 2, pp. 23-211, 2010.
- [5] A. D. D. Dwivedi and P. Chakrabarti, "Analytical modelling and ATLAS simulation of N+-Hg_{0.69}Cd_{0.31}Te/ n⁰-Hg_{0.78}Cd_{0.22}Te/ p+-Hg_{0.78}Cd_{0.22}Te p-i-n photodetector for longwevelength free space optical communication", *Optoelectronics and Advance Materials- Rapid Communication*, vol. 4, No. 4, pp. 480-497, 2010.
- [6] Reza Nasiri Mahalati and Joseph M. Kahn, "Effect of fog on free-space optical links employing imaging receivers", *Optical express*, Vol. 20 No. 2, pp. 1694-1661, 2012.
- [7] A. Rogalski, "New trends in semiconductor infrared detectors", *Opt. Engg.*, Vol. 33, pp. 1395-1412, 1994.
- [8] Krier, H.H. Gao and V.V. Sherstnev, "Room temperature InAs_{0.89} Sb_{0.11} photodetectors for CO detection at 4.6 μ m", *Applied Phys. Lett.*, Vol.77 (6), pp. 872- 874, 2000.
- [9] P. Chakrabarti, Senior Member IEEE, A. Krier, and A. F. Morgan, "Analysis and Simulation of a Mid-Infrared P+-InAs_{0.55}Sb_{0.15}P_{0.30}/n⁰-InAs_{0.89}Sb_{0.11}/N+-InAs_{0.55}Sb_{0.15}P_{0.30} Double Heterojunction Photodetector Grown by LPE", *IEEE Trans. on Electron Devices*, vol. 50, pp. 2049-2058, 2003.
- [10] Mohammad Nadimi and Alo Sadr, "Modeling and Simulation of High Operating Temperature MWIR Photodetector Based on Mercury Cadmium Telluride", *International Journal of Computer and Electrical Engineering*, vol. 3, No. 4, pp. 597-599, 2011.
- [11] R.J. McIntyre, "Multiplication noise in uniform avalanche diode", *IEEE Trans. Electron Devices*, 13, pp. 164-168, 1966.
- [12] R.J. McIntyre, "The distribution of gains in uniformly multiplying avalanche photodiodes: Theory", *IEEE Trans. Electron Devices*, ED19, pp. 703-713, 1972.
- [13] Y. Okuto and C. R. Crowell, "Energy conservation consideration in the characterization of impact ionization in semiconductors", *Phys. Rev. B*, vol. 6, pp. 3076-3081, 1972.
- [14] R. J. McIntyre, "Ionization coefficients in semiconductors: A nonlocal property", *Phys. Rev. B*, vol. 10, pp. 4284–4296, 1974.
- [15] R. J. McIntyre, "Threshold energy effect on avalanche breakdown voltage in semiconductor junctions", *Solid-State Electron.*, vol. 18, pp. 161–168, 1975.
- [16] G.E. Stillman, C.M. Wolfe, J.O. Dimmock, in *Semiconductors & Semimetals*, Vol. 12, published by Academic Press (New York), 1977.
- [17] R.J. McIntyre, "A new look at impact ionization-Part-I: a theory of Gain, Noise, Breakdown Probability, and Frequency response," *IEEE Trans. Electron Devices*, vol. 46, pp. 1623-1631, 1999.
- [18] M. Levinshtein, S. Rumyantsev, and M. Shur: "Hand book series on Semiconductor Parameters," *World Scientific*, vols. 1 & 2, Singapore, 1996.